CrossMark

Symmetry lowering and surface elasticity effects on Young's modulus and Poisson's ratio of nanofilms

Jiangang Li[1] · Bai Narsu[2] · Guohong Yun[2,3] · Aoxuan Wang[4] · Zhixiang Gao[1]

Abstract
Physical and mechanical properties of nanosized materials and structures are strongly affected by surface effects. In this paper, a self-consistent theoretical scheme for describing the elastic properties of nanofilms was proposed. The Young's modulus, biaxial modulus and Poisson's ratio of nanofilms were obtained analytically with considerations of symmetry lowering, surface elasticity, elastic parameter splitting and additional elastic coefficient. Applications of present theory to elastic systems such as Si nanofilm Young's modulus, Cu nanofilm biaxial modulus and Poisson's ratio yield good agreement with previous calculated results. We found that Young's modulus and Poisson's ratio were split due to symmetry lowering, and this splitting confirms the symmetry lowering. For a nanofilm with a given thickness, Young's modulus and biaxial modulus increase with surface elastic coefficients increase except $c_{12}^{\alpha,s}$. The larger positive $c_{12}^{\alpha,s}$ drives Young's modulus towards smaller abnormally. The present study in this paper is envisaged to provide useful insights for the design and application of nanofilm-based devices.

1 Introduction

Over the past decade, the mechanics of nanostructures has attracted a lot of attention due to their widely proposed applications in nanoelectromechanical systems (NEMS)

✉ Jiangang Li
lijiangang1127@163.com

✉ Zhixiang Gao
674496407@qq.com

1 School of Physics and Electronic Science, Shanxi Datong University and Shanxi Province Key Laboratory of Microstructure Electromagnetic Functional Materials, 037009 Datong, People's Republic of China

2 College of Physics and Electronic Information, Inner Mongolia Normal University and Inner Mongolia Key Laboratory of Physics and Chemistry of Functional Materials, 010022 Hohhot, People's Republic of China

3 Inner Mongolia Key Lab of Nanoscience and Nanotechnology and School of Physical Science and Technology, Inner Mongolia University, 010021 Hohhot, People's Republic of China

4 Committee of the Communist Youth League, Shanxi Datong University, 037009 Datong, People's Republic of China

[1–6]. As a result of large surface-to-volume ratio, mechanical properties including Young's modulus, biaxial modulus as well as Poisson's ratio of nanostructures are very different from their bulk counterparts [7–12]. And the role of the surface energy on the statics, buckling, postbuckling, and vibrations of metallic nanowires used for carrying electrical current have been displayed by Kiani [13–17].There are a great amount of works focused on the nanostructure elastic characters including experimental measurements, simulated calculations, and theoretical analyses [12, 18, 19]. Experimentally, researchers studied the size-dependent Young's modulus of Silicon (Si) nanofilms and confirmed decrease trend with decreasing film thickness [19]. The similar trend is also found in chromium (Cr) and gallium nitride (GaN) nanostructures [19–21]. While for some other nanostructures, Young's modulus has trend to increase with decreasing structure size, such as cupric oxide (CuO), zinc oxide (ZnO), silver (Ag) and tellurium (Te) [22–25]. Simulated calculation is another method for researching elasticity of nanostructures. Si Young's modulus was studied using molecular dynamics (MD) calculation [10]. Embedded-atom-method (EAM) was used for calculating FCC aluminium (Al) and Stillinger–Weber model was used for Si [26]. Copper (Cu) Young's modulus and Poisson's ratio were also studied by molecular dynamics (MD) calculation [12, 27].

Theoretically, a popular surface elastic theoretical scheme was to invent a surface elasticity concept in which the surface area was treated as a two-dimensional slice without thickness but with elastic characters. Miller and Shenoy studied size-dependent elasticity of nanostructures using this concept [26]. This surface elasticity theory gave the basic rule of surface effect on the elastic properties of nanofilms, i.e., surface modification and size dependence of nanofilm elasticity. A lot of works modeled mechanics of nanostructures within this scheme [28, 29]. Under this scheme, a nanostructure was seen as a hybrid structure, and was divided into a surface slice which is bonded on the bulk like core phenomenologically. This scheme was called as core-surface model. Chen et al. and Stan et al. developed core-surface model by introducing surface slice thickness [25, 30]. The developed hybrid structural surface elasticity model (hybrid model) was called as core–shell model. The core–shell model was modified by Yao et al. In modified core–shell model, a concept of mechanics inhomogeneity within surface slice was introduced to model surface elastic and piezoelectric properties [31, 32]. Following the hybrid scheme mentioned above, the size-dependent elasticity (Young's modulus) of nanostructure can be modeled via $Y_{\mathrm{eff}} = Y_{\mathrm{bulk}} + Y_s/t$ [18], here Y_{eff}, Y_{bulk} and Y_s are effective Young's modulus, bulk Young's modulus and surface Young's modulus of nanofilms, respectively. But for a nanofilm, besides surface elastic constants, the semi-two-dimensional structure makes crystallographic symmetry of the film reduce to lower one (the spherical symmetry reduces to cylindrical one for the case of isotropic hypothesis) [23]. Furthermore, the broken bond at surface relaxes and charge redistributes. This surface effect leads to overall structural relaxation in the film plane. On condition that the film plane is expanded, the vertical direction should be shrunk via Poisson's effect. In other words, the rotation symmetry of nanofilm is broken and translational symmetry along thickness direction is absent. Surface relaxation as well as symmetry lowering lead to differences of mechanical response between in-plane direction and vertical direction. Therefore, Young's modulus along vertical direction should be different from the in-plane direction counterpart. In addition, Poisson's effect should be also different for the case related to vertical direction. The surface modification of elasticity should be on elastic constants but rather than Young's modulus directly as hybrid model addressed. Then, a complex size-dependent Young's modulus appears. The symmetry lowering and surface relaxation, as well as surface elastic constants make the isotropic mechanical properties of isotropic materials be anisotropic and size dependent. The direct effects of symmetry lowering and surface relaxation are the split of the elastic coefficient C^γ and the appearance of an additional elastic constant $c_{12}^{\alpha,s}$ which is no bulk counterpart. This additional elastic constant accounts for the interaction between volume expansion and vertical lattice relaxation. It is very important to reckon in the elastic constant splitting as well as the additional elastic constant when modeling size-dependent elasticity of nanofilms [18, 33–35]. And these symmetry lowering effects finally induce anisotropic mechanical characters and split of Young's modulus and Poisson's ratio.

In this paper, we gave a universal elasticity strategy for mechanical properties of nanofilms. In the present theory, size-dependent Young's modulus, biaxial modulus and Poisson's ratio was deduced mathematically. The anisotropy of Young's modulus and Poisson's ratio was discussed in this work. The present elasticity theory strategy which includes Young's modulus, biaxial modulus and Poisson's ratio was established in this paper. As well as surface elasticity effect, symmetry lowering effect on nanofilm elastic property was discussed systematically. The present theory was applied to Si nanofilm Young's modulus, Cu nanofilm biaxial modulus and Poisson's ratio for the evidence of validity of the cylindrical theory in this paper.

2 Theory and models

2.1 The elastic free energy density of nanofilm

The elastic free energy density of a nanofilm with (001) surface under any deformations can be given by the following form according to du trémolet de lachersserie [33]

$$E_{\mathrm{el}} = \frac{1}{2}c_{11}^\alpha \left(\eta^{\alpha,1}\right)^2 + c_{12}^\alpha \eta^{\alpha,1}\eta^{\alpha,2} + \frac{1}{2}c_{22}^\alpha \left(\eta^{\alpha,2}\right)^2 + \sum_{\substack{\mu=\gamma,\delta \\ i=1,2}} \frac{1}{2}c^\mu \left(\eta_i^\mu\right)^2.$$

(1)

The strains η_i^μ ($\mu = \alpha,\ \gamma,\ \delta$ and $i = 1,\ 2$) are defined as follows [18, 34],

$$\eta^{\alpha,1} = \frac{1}{\sqrt{3}}\left(\varepsilon_{xx} + \varepsilon_{yy} + \varepsilon_{zz}\right),\ \eta^{\alpha,2} = \sqrt{\frac{2}{3}}\left(\varepsilon_{zz} - \frac{\varepsilon_{xx} + \varepsilon_{yy}}{2}\right),$$

$$\eta_1^\gamma = \frac{1}{\sqrt{2}}\left(\varepsilon_{xx} - \varepsilon_{yy}\right),$$

$$\eta_2^\gamma = \sqrt{2}\varepsilon_{xy},\ \eta_1^\delta = \sqrt{2}\varepsilon_{yz},\ \eta_2^\delta = \sqrt{2}\varepsilon_{zx}.$$

(2)

where ε_{ij} ($i,\ j = x,\ y,\ z$) are strain components in Cartesian coordinate. The film is assumed to be elastically isotropic for the case of the corresponding bulk material (i.e., $2c' = c_{44}$ in Voigt notation). For a nanofilm with several nanometer thickness, the surface relaxation as well as symmetry lowering make the mechanical response along vertical direction be different from the in-plane direction counterpart. And as a result of this symmetry lowering effect, following five

Fig. 1 (color online) Schematic of the nanofilm structure. The z direction is fixed perpendicular to the film plane and x–y plane is parallel to film plane
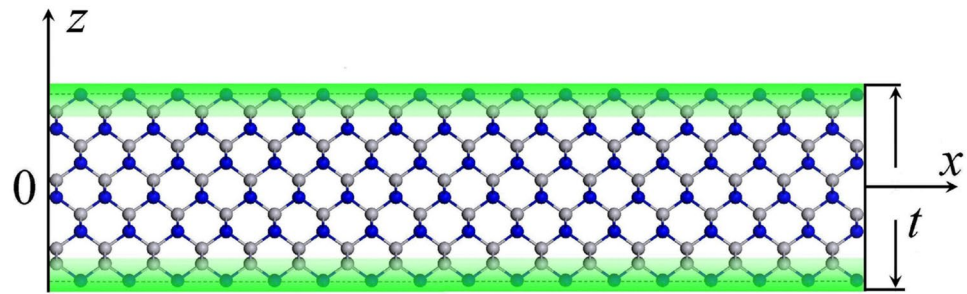
elastic constants are needed to fully describe the mechanical properties of nanofilms [18, 33],

$$c_{11}^\alpha = C^\alpha + \frac{2}{t_f}c_{11}^{\alpha,s}, \ c_{12}^\alpha = \frac{2}{t_f}c_{12}^{\alpha,s}, \ c_{22}^\alpha = C^\gamma + \frac{2}{t_f}c_{22}^{\alpha,s},$$
$$c^\gamma = C^\gamma + \frac{2}{t_f}c^{\gamma,s}, \ c^\delta = C^\gamma + \frac{2}{t_f}c^{\delta,s}. \tag{3}$$

where t_f is thickness of the film, and the elastic parameters $C^\alpha = c_{11} + c_{12}$, $C^\gamma = c_{11} - c_{12}$. In Eq. (3), one can find that C^α is simply modified by surface elastic parameter and film thickness while C^γ is split into three different elastic parameters. The additional elastic parameter $c_{12}^{\alpha,s}$ appears due to symmetry lowering (Fig. 1).

2.2 The in-plane direction Young's modulus and the corresponding Poisson's ratio

The nanofilms are stress-free in their vertical direction in that they are always grown on a substrate. Hence, we have a relation that $\sigma_{yz} = \sigma_{zx} = \sigma_{zz} = 0$. The strains ε_{yz}, ε_{zx} and ε_{zz} were given by Eqs. (A.2). Substituting ε_{yz}, ε_{zx} and ε_{zz} into Eq. (1), the elastic free energy can be written under the deformations parallel to the film plane (in-plane deformations) as

$$E_{el} = \frac{1}{4}Y'(\varepsilon_{xx} + \varepsilon_{yy})^2 + \frac{1}{4}c^\gamma(\varepsilon_{xx} - \varepsilon_{yy})^2 + c^\gamma\varepsilon_{xy}^2. \tag{4}$$

Where,

$$Y' = 3\frac{c_{11}^\alpha c_{22}^\alpha - \left[c_{12}^\alpha\right]^2}{c_{11}^\alpha + 2\sqrt{2}c_{12}^\alpha + 2c_{22}^\alpha}, \tag{5}$$

is biaxial modulus of nanofilms.

According to the Taylor series expanded form of biaxial modulus Eqs. (B.1) and (B.2), one can easily find that $Y'^{(0)} = Y/(1 - v)$ is biaxial modulus of bulk material from the definition given above. Here $Y = (c_{11} + 2c_{12})(c_{11} - c_{12})/(c_{11} + c_{12})$ and $v = c_{12}/(c_{11} + c_{12})$ stand for Young's modulus and Poisson's ratio of bulk material. To the first order of $1/t$,

the biaxial modulus is $Y'(t) \approx Y'^{(0)} + Y'^{(1)}/t$. This first order approximation is similar to hybrid surface model addressed. Hence the hybrid surface model can be seen as the first-order approximation of our theory.

To get Young's modulus and Poisson's ratio, we assume the stress is applied along x direction while keeping y direction stress free, i.e., $\sigma_{yy} = 0$. One can obtain

$$\varepsilon_{yy} = -\frac{Y' - c^\gamma}{Y' + c^\gamma}\varepsilon_{xx} = -v_{xy}\varepsilon_{xx}, \tag{6a}$$

$$\sigma_{xx} = \frac{2c^\gamma Y'}{Y' + c^\gamma}\varepsilon_{xx} = Y\varepsilon_{xx}. \tag{6b}$$

And then, the perpendicular direction strain ε_{zz} can be given using Eq. (A.2b) and Eq. (6a) as

$$\varepsilon_{zz} = -\frac{1}{2}v_b(1 - v_{xy})\varepsilon_{xx} = -v_{xz}\varepsilon_{xx}. \tag{7}$$

In the above equations, coefficients v_{xy}, v_{xz} and Y are Poisson's ratio of x-to-y direction, Poisson's ratio of x-to-z direction, and Young's modulus along in-plane direction, respectively. They are defined as

$$v_{xy} = \frac{Y' - c^\gamma}{Y' + c^\gamma}, \tag{8}$$

$$v_{xz} = \frac{1}{2}v_b(1 - v_{xy}), \tag{9}$$

$$Y = \frac{2c^\gamma Y'}{Y' + c^\gamma}. \tag{10}$$

The v_{xy} has the physical significance reads, that y direction strain is induced by x direction stress via Poisson's effect, the corresponding Poisson's ratio is just v_{xy}, and the ratio between y and x direction strains is $-v_{xy}$. The similar physical significance of v_{xz} relates to z instead of y direction.

According to the Taylor series expanded form of Young's modulus Eqs. (B.3) and (B.4), one can find that the Young's modulus of nanofilms is not simply $1/t$ size dependent. The

higher order (at least second order) terms are always important for ultrathin nanofilms with several nanometer thickness [18]. Equation (B.4) indicate that the surface elastic modification terms are structured by coupling surface and bulk elastic constants. Actually, the symmetry lowering and the construction of elastic constants but not Young's modulus inevitably introduce the complex coupling between surface and bulk elastic constants. This size-dependent trend is very different from simple $1/t$ dependence of the hybrid model.

2.3 The perpendicular direction of Young's modulus and the corresponding Poisson's ratio

If the stress is applied along z direction, i.e., perpendicular direction while keeping in-plane directions stress free, for a free-standing film, one can obtain the perpendicular direction Young's modulus and the corresponding Poisson's ratio. In this condition, the in-plane strains and stresses are isotropic because of that the isotropic property is still kept along in-plane directions while the symmetry is broken down along the perpendicular direction. The z direction stress σ_{zz} was given by Eq. (A.4).

The relation between perpendicular and in-plane direction strains can be obtained from Eq. (A.6) as

$$\varepsilon = -v_{zx}\varepsilon_{zz}, \tag{11}$$

$$v_{zx} = \frac{c_{11}^{\alpha} + \left(\sqrt{2}\big/2\right)c_{12}^{\alpha} - c_{22}^{\alpha}}{2c_{11}^{\alpha} - 2\sqrt{2}c_{12}^{\alpha} + c_{22}^{\alpha}}. \tag{12}$$

where v_{zx} is Poisson's ratio relates to the Poisson's effect from perpendicular to in-plane directions. It should be mentioned that v_{zx} is different from the Poisson' ratio v_{xz} as was discussed above, while v_{xz} is related to the Poisson's effect from in-plane direction to perpendicular direction. Substituting Eq. (11) into Eq. (A.5), one can obtain the relation between stress and strain along z direction as

$$\sigma_{zz} = Y_{zz}\varepsilon_{zz}, \tag{13}$$

$$Y_{zz} = \frac{1}{3}\left\{ \left(c_{11}^{\alpha} + 2\sqrt{2}c_{12}^{\alpha} + 2c_{22}^{\alpha}\right) - 2\frac{\left[c_{11}^{\alpha} + \left(\sqrt{2}\big/2\right)c_{12}^{\alpha} - c_{22}^{\alpha}\right]^{2}}{2c_{11}^{\alpha} - 2\sqrt{2}c_{12}^{\alpha} + c_{22}^{\alpha}} \right\}, \tag{14}$$

where Y_{zz} is Young's modulus along z direction. The elastic characters along perpendicular direction behave differently from in-plane directions due to symmetry lowering and surface relaxation. Hence, there are two Young's modulus and three Poisson's ratio coefficients to interpret the different elastic properties along perpendicular and in-plane directions elastic response. When comparing a nanofilm with its bulk counterpart, one observed that biaxial modulus is simply modified by surface elastic constants while uniaxial Young's modulus is split into two and Poisson's ratio is split into three different coefficients due to surface relaxation and symmetry lowering.

3 Results and discussions

The relative number of atoms that are bonded surface or interface increases with film thickness decreasing. And then surface elastic constants strongly affect the overall mechanical properties of nanofilms [36]. The broken bond at surface relaxes and the dangling bonds combine together. This effect induces atoms to move and depart from their customary position. Lattice structure and interatomic forces near the surface are changed. This surface reconstruction changes the elastic constant and Young's modulus at surface. Furthermore, the movement of surface atoms leads to surface stress and expands (or shrinks) the film in the film-plane. The film relaxes inward (or outward) along vertical direction due to Poisson's effect. The overall film is relaxed by the whole procedure of surface relaxation and surface reconstruction. And then, the symmetry of the film is broken and reduced. Therefore, Young's modulus and Poisson's ratio are strongly size-dependent when film thickness shrinks to several nanometers to form a nanofilm. Surface relaxation and symmetry lowering enhance the surface effect and make elastic properties of nanofilms be different from the corresponding bulk materials. The validity should be examined by comparing our theoretical solutions with relevant numerical computations as well as previous continuity theoretical work. Imitate the bulk elastic parameter relations $C^{\alpha} = c_{11} + 2c_{12}$, $C^{\gamma} = c_{11} - c_{12}$, the surface elastic parameter relations may be similar as

$$c_{11}^{\alpha,s} \approx c_{11}^{s} + 2c_{12}^{s}, \ c_{22}^{\alpha,s} \approx c_{11}^{s} - c_{12}^{s}, \ c^{\gamma,s} \approx c_{11}^{s} - c_{12}^{s},$$

but not exactly. Here '$\approx$' instead of '$=$' is used in the equations due to symmetry lowering of nanofilms. For a nanofilm, bulk modulus C^{α} is simply modulated by surface elasticity and film size (thickness exactly) while tetragonal modulus C^{γ} is split into two different parameters, i.e., tetragonal shear moduli along vertical direction c_{22}^{α} and in film plane c^{γ} (there are no shear strains for the case of simple epitaxy in this paper and the corresponding rhombohedral parameter c^{δ} is neglected here). If ignored the lowered symmetry, there should be relationship $c_{22}^{\alpha} = c^{\gamma}$ about the elastic coefficients like bulk materials. But the lowered symmetry induces the discrepancy between c_{22}^{α} and c^{γ}. This effect may result in different trends of size dependency between these two tetragonal shear moduli. Another symmetry lowering

effect is the additional elastic parameter c_{12}^{α} which is no bulk counterpart. This additional elastic parameter is along with the coupling between isotropic volume expansion and vertical lattice relaxation. This coupling means minus energy term in total elastic energy when the stress is applied along in-plane direction. And the minus energy term causes larger strain induced by the stress. Hence, the larger positive $c_{12}^{\alpha,s}$ drives Young's modulus towards smaller. The same procedure of $c_{12}^{\alpha,s}$ dependence also suits biaxial modulus. For example, Si film is softened by surface effect and surface elastic constant $c_{12}^{\alpha,s}$ is 27 N m^{-1} is shown in Table 1. Table 2 listed Si and Cu surface elastic parameters from simulated calculations in references [37, 38] for comparison. The symmetry lowering was not considered in references [37, 38] hence the notation of the surface elastic is different from present theory in this paper.

Normalized effective Young's modulus of Si nanofilm is shown in Fig. 2. The theoretically calculated line using Eq. (10) shows excellent agreement with molecular dynamics (MD) simulation data. For silicon, bulk elastic coefficients are $c_{11} = 165$ GPa, $c_{12} = 63$ GPa [36], and surface elastic coefficients are shown in Table 1. The hybrid model, i.e., $Y_{eff} = Y_{bulk} + Y_s/t$, result is also shown in Fig. 2. The surface Young's modulus in hybrid model was set as -20 N m^{-1} for comparison (see dashed line in Fig. 2). For hybrid model, larger (minus) surface Young's modulus induces obvious discrepancy between theory and simulated calculation for relatively thicker film ($t > 3$ nm), and on the other hand, smaller (minus) surface Young's modulus induces obvious discrepancy between theory and simulated calculation for relatively thinner film ($t < 3$ nm). The hybrid model holds different dependency (slope) on thickness compared with simulation. This difference originates from the lack of consideration of symmetry lowering for nanofilms. Generally speaking for a nanofilm with a certain thickness, Young's modulus increases with the larger positive surface elastic coefficients except $c_{12}^{\alpha,s}$. To clarify the $c_{12}^{\alpha,s}$ effect on nanofilm elastic characters, we plotted Si film $c_{12}^{\alpha,s}$ dependence of

Young's modulus with different film thickness in Fig. 3. The obvious trend of the lines in Fig. 3 is that Young's modulus decreases with larger positive $c_{12}^{\alpha,s}$ and this influence is enhanced by smaller film thickness.

In Fig. 4, we plotted Cu nanofilm biaxial modulus versus film thickness t and compared our theory with previous theory in reference [11]. Bulk elastic coefficients of Cu film are $c_{11} = 176.2$ GPa, $c_{12} = 124.9$ GPa, respectively [35, 39], and surface elastic coefficients were shown in Table 1. Solid line in Fig. 4 was plotted using Eq. (5), and continuum mechanics calculated data of other group from reference [11] was also shown in the figure for comparison (square symbol). Our theoretical calculation excellently agrees with the result from reference [11]. Follow Si nanofilm Young's modulus,
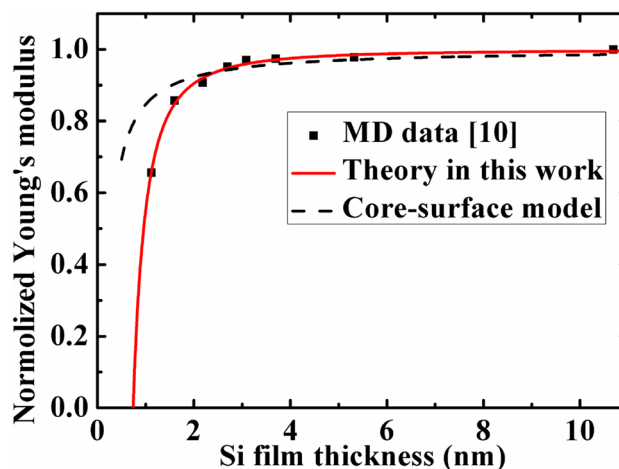

Fig. 2 (color online) Normalized Young's modulus of Si nanofilms. The red (dark grey) solid line is current theoretical calculation from Eq. (10). The dark dashed line is hybrid theoretical calculation. The molecular dynamics simulation (MD) data were from reference [10]
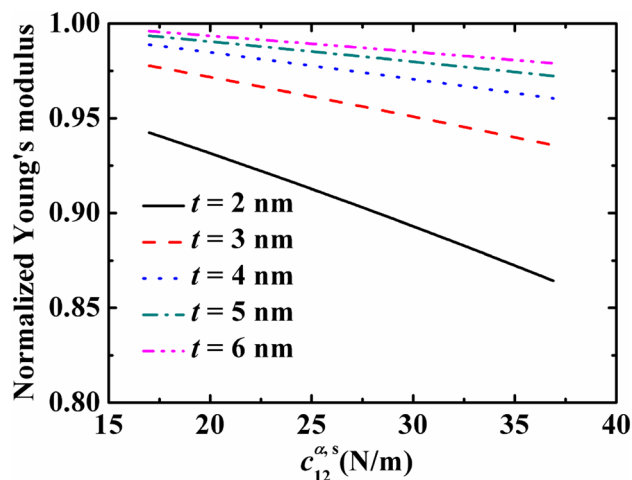
Table 1 Surface elastic parameters in N m^{-1} of Si and Cu nanofilms in this paper

System	$c_{11}^{\alpha,s}$	$c_{22}^{\alpha,s}$	$c_{12}^{\alpha,s}$	$c^{\gamma,s}$
Si	-15	-30	27	18
Cu	20	15	-16	-5

Table 2 Surface elastic parameters in N m^{-1} of Si and Cu nanofilms in references [37, 38]

Films	$c_{11}^s (c_{22}^s)$	c_{12}^s	$c_{12}^{\alpha,s}$
Si	-7.13 ± 4.17	-4.93 ± 0.42	–
Cu	-4.16	4.30	–

Fig. 3 (color online) Normalized Young's modulus of Si nanofilms as $c_{12}^{\alpha,s}$ function. Young's modulus decreases with the larger positive $c_{12}^{\alpha,s}$
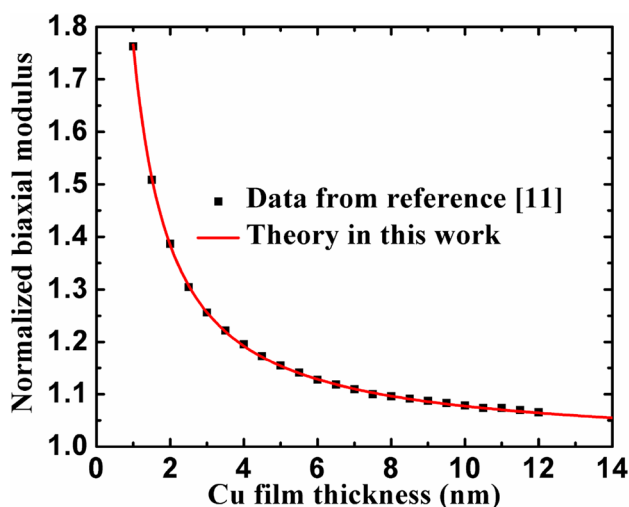
Fig. 4 (color online) Normalized biaxial modulus of Cu nanofilms versus film thickness. The square symbol data were from reference [11]
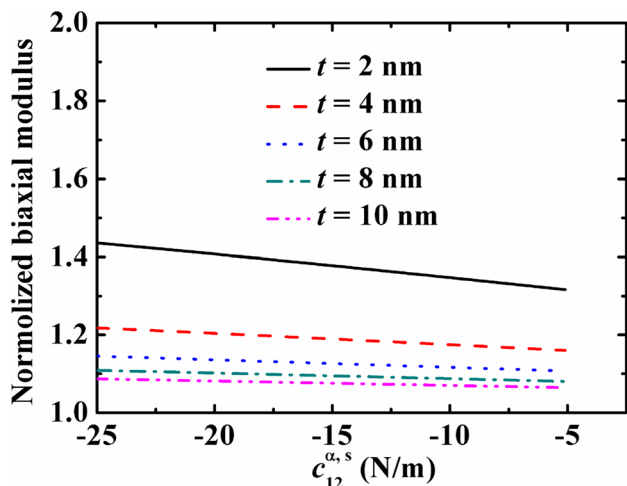

Fig. 5 (color online) Normalized biaxial modulus of Cu nanofilms versus $c_{12}^{\alpha,s}$. Biaxial modulus decreases with the larger positive $c_{12}^{\alpha,s}$

we plotted Cu nanofilm biaxial modulus as $c_{12}^{\alpha,s}$ function with different film thicknesses in Fig. 5. One can find that the dependence of $c_{12}^{\alpha,s}$ for Cu nanofilm biaxial modulus is very similar to Si film Young's modulus.

As well as Young's modulus and biaxial modulus, Poisson's ratio of nanofilm is also surface modulated and size dependent. Figure 6 plotted Cu nanofilm Poisson's ratio as function of film thickness using Eqs. (8), (9) and (12). Figure 6 shows that Poisson's ratio is split into three different parameters, v_{xy}, v_{xz} and v_{zx}. Symmetry lowering induced the different trends between three Poisson's ratio parameters as shown in Fig. 6. In film plane, Poisson's effect v_{xy} is enhanced by surface effect while the Poisson's effects relate to vertical direction v_{xz} and v_{zx} are weakened
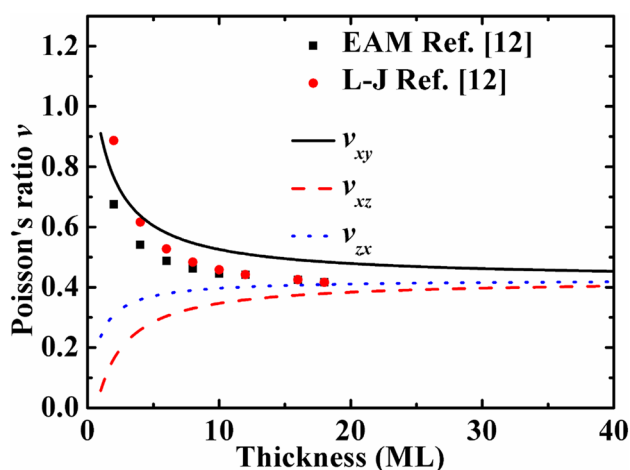

Fig. 6 (color online) Poisson's ratio of Cu nanofilms versus Cu monolayers. The embedded-atom-method (EAM) and Lennard-Jones (L-J) data were from reference [12]

by surface effect. The molecular dynamics (MD) simulations were brought into comparison with our present theoretical model. The dark square symbol is embedded-atom-method (EAM) potential calculation and red (dark grey) round symbol is Lennard-Jones (L-J) potential calculation. Both MD simulations in Fig. 6 were performed at 0 K [12]. This extreme temperature condition is the origin of the discrepancy between MD results and our present model calculation from Eq. (8).

4 Conclusions

In summary, the surface elastic coefficients affect the overall elastic response of nanofilms, while relaxation of broken bond and redistribution of charge at surface lowered the symmetry of nanofilms. This symmetry lowering splits elastic coefficient C^γ and introduces additional elastic coefficient c_{12}^α without bulk counterpart. The surface elasticity effect and symmetry lowering effect were reckoned in our model calculations. The applications of our model to Si and Cu nanofilms implied that the present model works well on the ultrathin nanofilms with several nanometers. To reveal the symmetry lowering effect and the additional surface elastic coefficient $c_{12}^{\alpha,s}$ effect on nanofilm elastic properties, this paper calculated curves of Young's modulus and biaxial modulus versus $c_{12}^{\alpha,s}$ with different film thicknesses. We found that larger positive $c_{12}^{\alpha,s}$ of nanofilm, not only Si but also Cu (actually any nanofilm material), driving Young's modulus (as well as biaxial modulus) towards smaller. The symmetry lowering induces the split of Young's modulus and Poisson's ratio. And the other way round, the split of Young's modulus and Poisson's ratio proved the lowered symmetry of nanofilms.

While core-surface model as well as core–shell model cannot present the symmetry lowering and the corresponding effects.

References

1. K. Kiani, Vibrations and instability of pretensioned current-carrying nanowires acted upon by a suddenly applied three-dimensional magnetic field. Mater. Chem. Phys. **162**, 531–541 (2015)
2. K. Kiani, Stability and vibrations of double parallel current-carrying nanowires immersed in a longitudinal magnetic field. Phys. Lett. A **379**, 348–360 (2015)
3. Y. Yao, S.-H. Chen, Surface effect in the bending of nanowires. Mech. Mater. **100**, 12–21 (2016)
4. Z. Yan, Modeling of a nanoscale flexoelectric energy harvester with surface effects. Physica E **88**, 125–132 (2017)
5. J.-J. Li, K.-D. Zhu, All-optical mass sensing with coupled mechanical resonator systems. Phys. Rep. **525**, 223–254 (2013)
6. W.-M. Zhang, K.-M. Hu, B. Yang, Z.-K. Peng, G. Meng, Effects of surface relaxation and reconstruction on the vibration characteristics of nanobeams. J. Phys. D: Appl. Phys. **49**, 165304 (2016)
7. J.-G. Guo, Y.-P. Zhao, The size-dependent elastic properties of nanofilms with surface effects. J. Appl. Phys. **98**, 274306 (2005)
8. J.-G. Guo, Y.-P. Zhao, The size-dependent bending elastic properties of nanobeams with surface effects. Nanotechnology **18**, 295701 (2007)
9. K. Kiani, Axial buckling analysis of a lender current-carrying nanowires acted upon by a magnetic field using the surface energy approch. J. Phys. D: Appl. Phys. **48**, 245302 (2015)
10. H. Sadeghian, J.F.L. Goosen, A. Bossche, B.J. Thijsse, F.V. Keulen, Effects of size and surface on the elasticity of silicon nanoplates: Molecular dynamics and semi-continuum approaches. Thin Solid Films **520**, 391–399 (2011)
11. R. Dingreville, J.-M. Qu, M. Cherkaoui, Surface free energy and its effect on the behavior of nano-sized particles, wires and films. J. Mech. Phys. Solids **53**, 1872–1854 (2005)
12. F.H. Streitz, K. Sieradzki, R.C. Cammarata, Elastic properties of thin fcc films. Phys. Rev. B **41**, 12285–12287 (1990) (R)
13. K. Kiani, Column buckling of magnetically affected stocky nanowires carrying electric current. J Phys. Chem. solids **83**, 140–151 (2015)
14. K. Kiani, Surface and shear energy effects on vibrations of magnetically affected beam-like nanostructures carrying direct currents. Int. J Mech. Sci. **113**, 221–238 (2016)
15. K. Kiani, Elastic buckling of current-carrying double-nanowire systems immersed in a magnetic field. Acta Mech. **227**, 3549–3570 (2016)
16. K. Kiani, A refined integro-surface energy-based model for vibration of magnetically actuated double-nanowire-system carrying electric current. Phys. E **86**, 225–236 (2017)
17. K. Kiani, Dynamic interactions between double current-carrying nanowires immersed in a longitudinal magnetic filed: Novel integro-surface energy-based models. Int. J Mech. Sci. **107**, 98–133 (2016)
18. J.-G. Li, B. Narsu, G.-H. Yun, H.-Y. Yao, Elasticity theory of ultrathin nanofilms. J. Phys. D Appl. Phys. **48**, 285301 (2015)
19. H. Sadeghian, C.-K. Yang, J.F.L. Goosen, A. Bossche, U. Staufer, P.J. French, F.V. Keulen, Effects of size defects on the elasticity of silicon nanocantilevers. J. Micromech. Miroeng. **20**, 064012 (2010)
20. S.G. Nilsson, X. Borrisé, L. Montelius, Size effect on Young's modulus of thin chromium cantilevers. Appl. Phys. Lett. **85**, 3555–3557 (2004)
21. C.-Y. Nam, P. Jaroenapibal, D. Tham, D.E. Luzzi, S. Evoy, J.E. Fischer, Diameter-dependent electromechanical properties of GaN nanowires. nano Lett. **6**, 53–158 (2006)
22. G.Y. Jing, H.L. Duan, X.M. Sun, Z.S. Zhang, J. Xu, Y.D. Li, J.X. Wang, D.P. Yu, Surface effects on elastic properties of silver nanowires: Contact atomic-force microscopy. Phys. Rev. B **73**, 235409 (2006)
23. E.P.S. Tan, Y. Zhu, T. Yu, L. Dai, C.H. Sow, V.B.C. Tan, C.T. Lim, Crystallinity and surface effects on Young's modulus of CuO nanowires. Appl. Phys. Lett. **90**, 163112 (2007)
24. G. Stan, S. Krylyuk, A.V. Davydov, M. Vaudin, L.A. Bendersky, Cook, R F, Surface effects on the elastic modulus of Te nanowires. Appl. Phys. Lett. **92**, 241908 (2008)
25. C.Q. Chen, Y. Shi, Y.S. Zhang, J. Zhu, Y.J. Yan, Size dependent of Young's modulus in ZnO nanowires. Phys. Rev. Lett. **96**, 075505 (2006)
26. R.E. Miller, V.B. Shenoy, Size-dependent elastic properties of nanosized structural elements. Nanotechnology **11**, 139–147 (2000)
27. A. Ahadi, S. Melin, Size dependence of the Poisson's ratio in single-crystal fcc cupper nanobeams. Comput. Mater. Sci. **111**, 322–327 (2016)
28. F. Hao, D.-N. Fang, Modeling of magnetoelectric effects in flexural nanobilayers: The effects of surface stress. J. Appl. Phys. **113**, 104103 (2013)
29. X. Liang, S.-L. Hu, S.-P. Shen, Effects of surface and flexoelectricity on a piezoelectric nanobeam. Smart. Mater. Struct. **23**, 035020 (2014)
30. G. Stan, C.V. Ciobanu, P.M. Parthangal, R.F. Cook, Diameter-dependent radial and tangential elastic moduli on ZnO nanowires. nano Lett **7**, 3691–3697 (2007)
31. H.-Y. Yao, G.-H. Yun, B. Narsu, J.-G. Li, Surface elasticity effect on the size-dependent elastic property of nanowires. J. Appl. Phys. **111**, 083506 (2012)
32. H.-Y. Yao, G.-H. Yun, B. Narsu, Influence of exponentially increasing surface elasticity on the piezoelectric potential of a bent ZnO nanowires. J. Phys. D: Appl. Phys. **45**, 285304 (2012)
33. du Rremolet de Lacheisserie E, Definition and measurement of the magnetoelastic coupling coefficients. Phys. Rev. B **51**, 15925 (1995)
34. du Rremolet de Lacheisserie E, Magnetostriction Theory and Applications of Magnetoelasticity (Boca Raton, FL CRC, 1993)
35. X. Lei, B. Narsu, G.-H. Yun, J.-G. Li, H.-Y. Yao, Axial buckling transverse vibration of ultrathin nanowires: low symmetry and surface elastic effect. J. Phys. D: Appl. Phys. **49**, 175305 (2016)
36. D. Sander, The correlation between mechanical stress and mechanic anisotropy in ultrathin films. Rep. Prog. Phys. **62**, 809–858 (1999)
37. S. Izumi, S. Hara, T. Kumagai, S. Sakai, A method for calculating surface stress and surface elastic constants by molecular dynamics: application to the surface of crystal and amorphous silicon. Thin Solid Films **467**, 253–260 (2004)
38. V.B. Shenoy, Atomic calculations of elastic properties of metallic fcc crystal surfaces. Phys. Rev. B **71**, 094104 (2005)
39. C. Kittel, *Introduction to Solid State Physics 7th edn* (Wiley, New York, 1997)